

Pairing fluctuations in the pseudogap state of copper-oxide superconductors probed by the Josephson effect

N. BERGEAL^{1*}, J. LESUEUR^{1*}, M. APRILI^{1,2}, G. FAINI³, J. P. CONTOUR⁴ AND B. LERIDON¹

¹Laboratoire Photons Et Matière - UPR5-CNRS, ESPCI, 10 Rue Vauquelin - 75005 Paris, France

²Laboratoire de Physique des Solides, Université Paris-Sud, 91405 Orsay, France

³Laboratoire de Photonique et de Nanostructures LPN-CNRS, Route de Nozay, 91460 Marcoussis, France

⁴Unité Mixte de Physique CNRS/THALES, (CNRS-UMR137) Route départementale 128, 91767 Palaiseau Cedex, France

*e-mail: nicolas.bergeal@yale.edu; jerome.lesueur@espci.fr

Published online: 29 June 2008; doi:10.1038/nphys1017

The phase diagram of high-temperature superconductors is still to be understood¹. In the low-carrier-doping regime, a loss of spectral weight in the electronic excitation spectrum—the so-called pseudogap—is observed above the superconducting temperature T_c , and below a characteristic temperature T^* (ref. 2). First observed in the spin channel by NMR measurements, the pseudogap has also been observed in the charge channel by scanning probe microscopy and photoemission experiments, for instance². An important issue to address is whether this phenomenon is related to superconductivity or to a competing ‘hidden’ order. In the superconductivity case, it has been suggested that superconducting pairing fluctuations may be responsible, but this view remains to be tested experimentally. Here, we have designed a Josephson-like experiment to probe directly the fluctuating pairs in the normal state. We show that fluctuations survive only in a restricted range of temperature above T_c , well below T^* , and therefore cannot explain the opening of the pseudogap at higher temperature.

Angle-resolved photoemission spectroscopy^{3,4} and scanning tunnelling spectroscopy⁵ showed a characteristic energy of the pseudogap that merges with the superconducting gap when the temperature is lowered below T_c . This reveals a smooth crossover rather than a sharp transition line between the pseudogap regime and the superconducting state, and has led to the superconducting precursor scenario. As opposed to the conventional Bardeen–Cooper–Schrieffer (BCS) transition, where pairing and condensation occur simultaneously at T_c , in underdoped cuprates fluctuating pairs may form at T^* , with no long-range coherence, and condense in the superconducting state at T_c (refs 6,7). Difficulties in confirming (or invalidating) this scenario arise from the fact that most of the experimental techniques used to investigate the pseudogap are sensitive only to the one-particle excitations, and therefore cannot provide a test of pairing above T_c . Owing to its ability to probe the properties of the superconducting wavefunction, the Josephson effect is a natural way to address the fluctuation issue.

In a second-order phase transition, the susceptibility is given by the linear response of the order parameter to a suitable external field. In the case of the superconducting phase transition, the

role of the external field can be played by the rigid pair field of a second superconductor below its own T_c (refs 8,9). In a Josephson junction in which one side of the junction is the fluctuating superconductor of interest above its T_c , whereas the other side is a superconductor below its T_c , the coupling between the pairing fluctuations and the well-established pair field gives rise to an excess current I_{ex} proportional to the imaginary part of the frequency- and wavenumber-dependent pair susceptibility $\chi(\omega, q)$. For a conventional superconductor above its T_c (ref. 9)

$$\chi^{-1}(\omega, q) = N(0)\varepsilon(1 - i\omega/\Gamma_0 + \xi^2(T)q^2),$$

where $\Gamma_0 = (16k_B/h)(T - T_c)$ is the relaxation rate of the fluctuations, $\xi(T)$ is the coherence length, $N(0)$ is the quasiparticle density of states and $\varepsilon = (T - T_c)/T_c$. The frequency is related to the d.c. bias voltage V across the junction through the Josephson relation $\omega = 2eV/\hbar$ and the wavenumber q is related to a magnetic field parallel to the junction. In the present experiments, the excess conductance rather than I_{ex} is measured. In the absence of magnetic field⁹, it can be expressed as:

$$G_{ex}(V) = A \frac{2e}{\hbar\Gamma_0\varepsilon} \frac{1 - (\omega/\Gamma_0)^2}{[1 + (\omega/\Gamma_0)^2]^2}, \quad (1)$$

where A depends on the coupling through the barrier and on the characteristics of the superconductors⁸. This d.c. measurement is sensitive to the pair fluctuations at any frequency (the voltage sets it) and its temperature dependence is only given by the distance to T_c through ε and Γ_0 .

In 1970, Anderson and Goldman observed gaussian fluctuations just above the T_c of conventional superconductors in good agreement with this model¹⁰. Janko *et al.* proposed a similar experiment, where the superconductivity of an optimally doped (OD) cuprate is used to probe the superconducting fluctuations in the pseudogap regime of an underdoped (UD) cuprate with a lower T_c (ref. 11). They predicted that an excess current in the junction should persist up to T^* if, according to their model, incoherent pairs are responsible for the pseudogap phase (or up to T_c^{OD} if $T^* > T_c^{OD}$). Independently of their respective theoretical

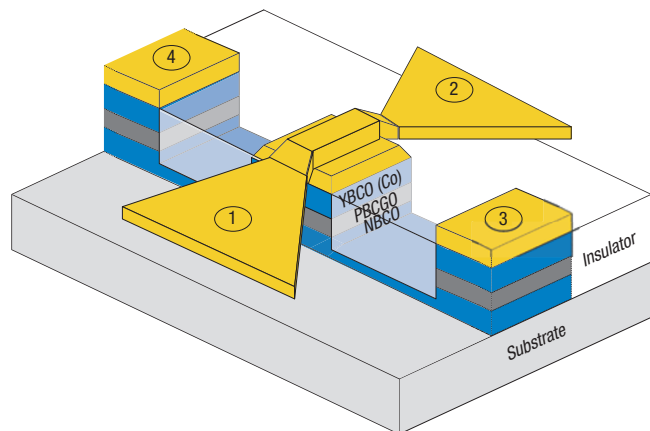


Figure 1 Trilayer junction. Schematic view of a *c* axis $\text{YBa}_2\text{Cu}_{2.8}\text{Co}_{0.2}\text{O}_7$ (100 nm) / $\text{PrBa}_2\text{Cu}_{2.8}\text{Ga}_{0.2}\text{O}_7$ (30 or 50 nm) / $\text{NdBa}_2\text{Cu}_3\text{O}_7$ (200 nm) junction. For the sake of clarity, the insulating part in front of the junction is not represented. Each junction is protected by an *in situ* gold layer and is connected with four electrodes (1 and 2 on the top, 3 and 4 at the bottom).

framework, the scenarios involving pairing fluctuations formed at T^* should lead to the same conclusion. On the contrary, for a standard BCS-like transition, the contribution of pairing fluctuations should be limited to the vicinity of T_c^{UD} .

Josephson-like structures required for this experiment involve two superconducting materials with different doping levels (optimally doped and underdoped) separated by a barrier. For this study, we made *c*-axis $\text{YBa}_2\text{Cu}_{2.8}\text{Co}_{0.2}\text{O}_7$ (underdoped) / $\text{PrBa}_2\text{Cu}_{2.8}\text{Ga}_{0.2}\text{O}_7$ / $\text{NdBa}_2\text{Cu}_3\text{O}_7$ (optimally doped) junctions with sizes ranging from $40 \times 40 \mu\text{m}^2$ to $5 \times 5 \mu\text{m}^2$ within a wafer (Fig. 1) (see the Methods section).

Figure 2a shows the resistance versus temperature curve of a typical junction. Below $T_c^{\text{OD}} = 90$ K (transition width $\Delta T_c^{\text{OD}} \approx 3$ K), the high resistance of the barrier (15Ω) and the equipotential gold layer ($150 \text{ m}\Omega$) on the top of the mesa guarantee that the current flows homogeneously along the *c* axis in the junction, and that the voltage drop measured in this experiment is dominated by the barrier. At around 60 K, the underdoped compound becomes superconducting as expected from the Co doping level, and Josephson coupling occurs between the two layers. As the temperature is lowered, the coupling becomes stronger than the thermal fluctuations and a clear Josephson critical current starts to rises up below 60 K (Fig. 2c). Given the resistive transition width ($\Delta T_c^{\text{UD}} \approx 5$ K), and the aim of the experiment to probe Josephson-like coupling above T_c^{UD} , we choose 61 K to be T_c^{UD} in the following. This is confirmed by SQUID magnetometry measurements on underdoped test samples (Fig. 2b).

Before describing the main temperature regime of interest ($61 \text{ K} \rightarrow 90 \text{ K}$), we first establish that both d.c. and a.c. Josephson effects do occur when both electrodes are in the superconducting state. This is of great importance because the excess current in the fluctuating regime has the same origin as the Josephson one at low temperature. Below T_c^{UD} , current–voltage characteristics exhibit a typical Josephson resistively shunted junction-like behaviour with an $I_c R_n$ product of 2 meV at 4.2 K (Fig. 3). The current–voltage characteristics exhibit clear Shapiro steps at fixed voltage $V_n = nfh/2e$ ($n = 0, \pm 1, \dots$) when the junction is irradiated with microwaves of frequency f (Fig. 3)¹². Such a Josephson effect through $\text{PrBa}_2\text{Cu}_3\text{O}_7$ (PBCO) (or $\text{PrBa}_2\text{Cu}_{2.8}\text{Ga}_{0.2}\text{O}_7$ (PBCGO)) barriers has been reported by several groups^{13,14}. This material is

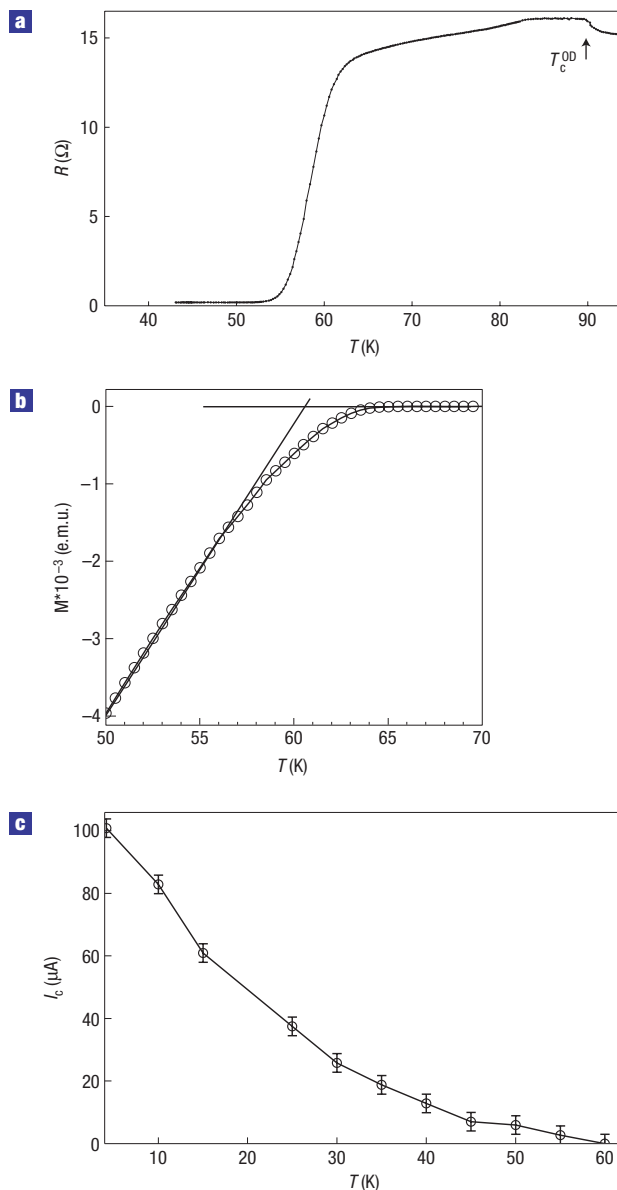


Figure 2 T_c of the trilayer junction. **a**, Resistance versus temperature of a $5 \times 5 \mu\text{m}^2$ junction made with a 30-nm-thick barrier. At $T_c^{\text{OD}} = 90$ K, the optimally doped electrode becomes superconducting, producing a weak current redistribution in the junction (see arrow). Below $T_c^{\text{UD}} \approx 61$ K, Josephson coupling occurs and the resistance drops. **b**, Magnetization versus temperature of a YBCO(Co) layer deposited on a PBCGO layer to reproduce the experimental condition of the trilayer growth. Extrapolation of the curve gives $T_c^{\text{UD}} = 61 \text{ K} \pm 1 \text{ K}$. **c**, Josephson critical current of the junction as a function of the temperature. Error bars originate from the rounding of the $I(V)$ curves with temperature.

known to contain localized states, which control the transport; the Josephson effect takes place by direct or resonant tunnelling through localized states in the barrier^{13–15}. At finite energy, quasiparticle transport occurs by hopping through these states^{16,17}. In our junction, the background conductance of a 30-nm-thick barrier has a weak dependence with energy for $T > T_c^{\text{OD}}$, as expected for one or two localized states in the barrier. The conductance follows the characteristic law $G = G_0 + \alpha V^{4/3}$, whereas junctions with a 50-nm-thick barrier exhibit the power law

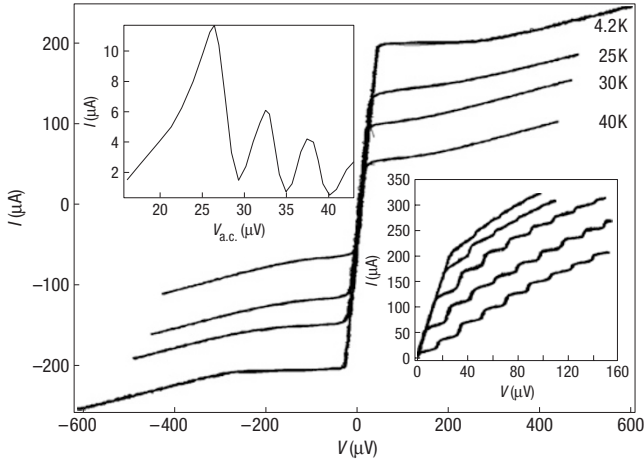


Figure 3 Current–voltage characteristics of a $10 \times 10 \mu\text{m}^2$ junction made with a 50-nm-thick barrier. At $T = 4.2 \text{ K}$, $I_c \approx 200 \mu\text{A}$ and $R_n \approx 10 \Omega$. The finite slope of the Josephson current is due to the gold layer resistance ($150 \text{ m}\Omega$) in series with the junction. I_c and R_n are found to scale with the area of the junction. Right inset: $I(V)$ characteristics of the junction under microwave radiation ($f = 8 \text{ GHz}$). Shapiro steps ($n = 0, 1, 2, 3$) appear when the radiation power is increased (from top to bottom). The width of the steps satisfies the linear relation with frequency $V_n = n\hbar/2e$. Left inset: Oscillation of the current height of the Shapiro step $n = 1$ as a function of the microwave voltage $V_{a.c.}$.

$G = G_0 + \alpha V^{4/3} + \beta V^{5/2}$ expected for three localized states (Fig. 4a, right inset). These energy dependencies of the conductance are weak, and show up mainly above 10 mV, well above the biases considered in the following. As the transport includes non-elastic hopping, no clear spectroscopic signatures are expected as opposed to the case in standard tunnel junctions. It must be stressed that for this Josephson-like experiment, several types of barrier can be suitable and not necessarily a tunnelling one.

We now focus on the intermediate temperature regime ($T_c^{\text{UD}} < T < T_c^{\text{OD}}$): the one of main interest here. To increase the sensitivity of the experiment, we measure the dynamic conductance $G = dI/dV$ of the junction as a function of the bias voltage V . Figure 4a shows typical results. An excess conductance peak emerges from the Josephson current at zero energy when the temperature crosses T_c^{UD} , and reduces rapidly when the temperature is increased further. It disappears 14 K above T_c^{UD} , below T_c^{OD} and therefore well below the characteristic temperature expected for the pseudogap in this compound ($T^* \approx 250 \text{ K}$). The peak presents all of the characteristics expected from standard gaussian fluctuations above T_c^{UD} as calculated and observed in conventional superconducting transitions¹⁰. The excess conductance peak is strongly suppressed by microwave radiation (Fig. 4a, left inset); this can be used to get a suitable background and extract the excess conductance due to fluctuations. Figure 4b shows the excess conductance as a function of the bias voltage (bottom axis) and the corresponding pulsation ω (top axis) at two different temperatures. The overall shape of the curves is in good agreement with the excess conductance computed from equation (1) (solid lines), provided the phase fluctuations introduced by Johnson noise in this rather high-temperature experiment are properly taken into account. Γ_0 has to be replaced by $\Gamma = \Gamma_0 + \Gamma_1$, where $\Gamma_1 = 4e^2 R k_B T / \hbar^2$ and R is the resistance of the junction¹⁸. In this case, the low-frequency part of the fluctuation spectrum (corresponding to $\Gamma_0 < \Gamma_1$) is cut off by thermal noise. The relaxation rates of fluctuations Γ_0 are found to be $3.25 \times 10^{12} \text{ rad s}^{-1}$

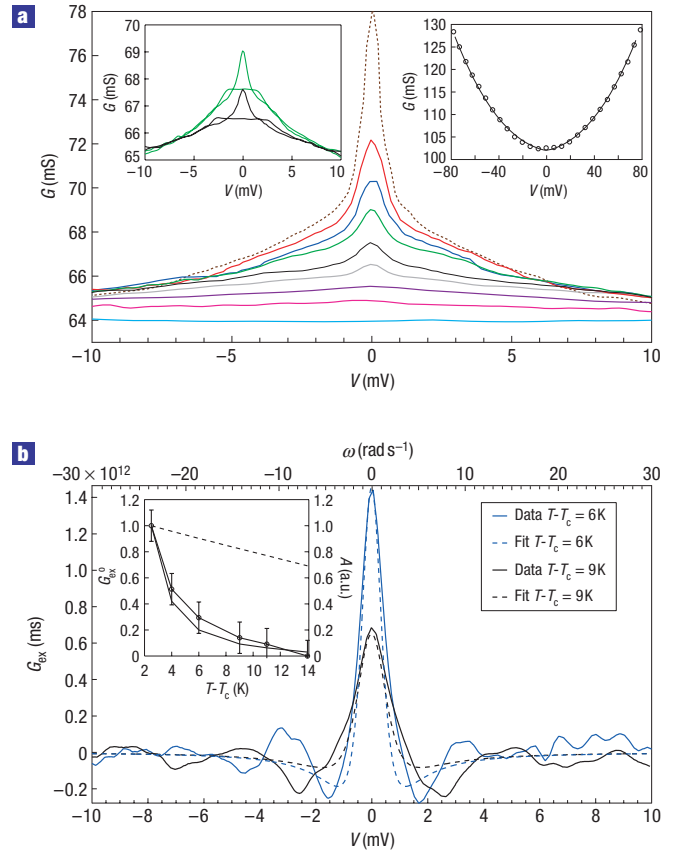


Figure 4 Conductance of the junction above T_c^{UD} . **a**, Conductance as a function of voltage of a $5 \times 5 \mu\text{m}^2$ and 30-nm-thick junction, corresponding to (from top to bottom): $T - T_c^{\text{UD}} = 0$ (dotted line), 2.5 K, 4 K, 6 K, 9 K, 11 K, 14 K, 20 K, 22 K. Left inset: $G(V)$ at $T - T_c^{\text{UD}} = 6 \text{ K}$ (green line) and 9 K (black line) with and without microwave radiation applied. Right inset: Experimental $G(V)$ of a $10 \times 10 \mu\text{m}^2$ and 50-nm-thick junction (circles) fitted by the power law $G = G_0 + \alpha V^{4/3} + \beta V^{5/2}$ (solid line). **b**, Excess conductance G_{ex} as a function of voltage and the corresponding frequency $\omega = 2eV/\hbar$ (top axis) at $T - T_c^{\text{UD}} = 6 \text{ K}$ and 9 K. Solid lines correspond to experimental data and dashed lines to the computed G_{ex} where the coefficient A is set by the fit of G_{ex} at $T - T_c^{\text{UD}} = 6 \text{ K}$. In this simulation, we use $R_n \approx 15 \Omega$ and $C = 1.4 \times 10^{-14} \text{ F}$ to take into account the thermal noise¹⁴. Inset: Temperature dependence of the computed normalized excess conductance at $V = 0$ (solid line), experimental normalized excess conductance (circles) and the coupling factor A according to ref. 8 (dashed line). As A is calculated in the tunnelling limit, a slightly different temperature dependence may be expected in the case of a weak insulating barrier. The error bars originate from the uncertainty on the background subtraction.

at $T - T_c^{\text{UD}} \approx 6 \text{ K}$ and $3.9 \times 10^{12} \text{ rad s}^{-1}$ at $T - T_c^{\text{UD}} \approx 9 \text{ K}$ close to the expected value from the gaussian model ($2.1 \times 10^{12} \text{ rad s}^{-1}$ and $3.1 \times 10^{12} \text{ rad s}^{-1}$), albeit a little bit larger by a factor 2. This small discrepancy may originate from the details of the transport (localized states, d-wave symmetry of the superconducting order parameter and so on), and the actual choice of T_c^{UD} . In the proposal of Janko *et al.*¹¹, the extra contribution due to fluctuating pairs is expected to be asymmetric in voltage and to move towards high energy when the temperature is increased: none of these predictions is observed here. The broad feature, which extends up to 10 meV, is seen in all of the samples but cannot be attributed to fluctuations because it is already observed at low temperature (where no fluctuations are present) and evolves continuously through T_c^{UD}

up to T_c^{OD} , where it disappears. Following ref. 19, we therefore attribute this feature to Andreev reflection in the presence of localized states.

The excess current is observed in the temperature range where gaussian fluctuations are expected to take place in cuprates, that is, roughly 15 K above T_c^{UD} given their short coherence length and the rather weak anisotropy of $\text{YBa}_2\text{Cu}_3\text{O}_{6+x}$ (YBCO) compounds. As an example, the Lawrence–Doniach calculation of the paraconductivity above T_c leads to less than 5% of excess conductivity in this range. As the temperature dependence of the pairing peak is a key point, other possible contributions have to be discussed. We can exclude any contribution of the underdoped layer itself because the c -axis conductance of underdoped YBCO increases with temperature in this temperature range²⁰, and because no specific energy dependence is expected. In this linear-response experiment, the current is directly proportional to $\text{Im}\chi$, which is independent of the strength of the external field. However, the rigid pair field of the optimally doped layer decreases when approaching T_c^{OD} , and so does the excess current through the parameter $A(T)$ in equation (1) (ref. 8). But in the range of interest here, $A(T)$ varies slowly as compared with the strong decrease of the conductance peak height (Fig. 4b, inset). Taking it into account nevertheless, we carried out a full calculation of $G_{\text{ex}}(V=0)$ according to equation (1) and compared it with the data (Fig. 4b, inset). The good agreement indicates that gaussian fluctuations dominate the decay of superconductivity above T_c^{UD} .

The only other attempt to (indirectly) detect pairing above T_c in underdoped cuprates reported in the literature²¹ is a high-frequency measurement done on $\text{Bi}_2\text{Sr}_2\text{CaCu}_2\text{O}_{8+\delta}$ compounds in a restricted range of frequency, and interpreted within a precise theoretical framework based on the Kosterlitz–Thouless physics. Fluctuations have been observed only up to 95 K, far below T^* , in rather good agreement with our result. The strength of our experiment is that it relies only on the presence of pairing fluctuations and the Ginsburg–Landau theory. Thus, it can demonstrate directly the presence of gaussian fluctuations in a broad band of frequency, with no further theoretical assumption.

A popular set of experiments supporting non-gaussian pairing fluctuations in the pseudogap regime is the observation of a large Nernst signal well above T_c^{UD} in underdoped $\text{La}_{2-x}\text{Sr}_x\text{CuO}_4$ (ref. 22) and $\text{Bi}_2\text{Sr}_2\text{CaCu}_2\text{O}_{8+\delta}$ (refs 22,23) compounds, attributed to vortex-like excitations. However, the same experiments carried out on underdoped YBCO clearly show that in this rather clean material, the corresponding range of temperature is reduced to a value compatible with our result²⁴ (typically 10 K above T_c^{UD}) and expands when the disorder is increased. At this point, we would like to mention that a recent calculation²⁵ and experiments²⁶ on dirty BCS superconductors do show that a Nernst signal originating from gaussian fluctuations can be measured well above T_c .

METHODS

Josephson-like structures involving two different materials have to be made with thin films. As high- T_c compounds grow at high temperature where diffusion is fast, underdoping cannot be obtained by changing the oxygen concentration in only one layer. For the coupling to be strong enough, interfaces have to be of very high quality, and therefore an epitaxial structure has to be used: the barrier must have the same crystallographic structure as the superconductors. Only a few materials can fulfil these requirements. We have chosen: (1) $\text{NdBa}_2\text{Cu}_3\text{O}_7$ (NdBCO) as the optimally doped compound because it grows smoother than the yttrium compound; (2) $\text{YBa}_2\text{Cu}_{2.8}\text{Co}_{0.2}\text{O}_7$ (YBCO(Co)) as the underdoped material: Co substitutes Cu in the chains, leading to underdoping with minor

disorder in the CuO_2 planes²⁷; (3) PBCGO as the barrier: PBCO is a weak insulator, and doping with Ga increases its resistivity. Doping PBCO with Ga reduces the number of localized states. Therefore, we can grow thick barriers to avoid microshorts while keeping the number of localized states low. For this experiment, we used mainly 30- and 50-nm-thick barriers. c -axis trilayer structures YBCO(Co)/PBCGO/NdBCO have been grown on SrTiO_3 (100) substrates by pulsed laser deposition and covered by an *in situ* gold layer. Lithography and a high-energy (250 keV) ion irradiation technique through an *in situ* gold mask have been used to design trilayer junctions²⁸.

Standard four-probe measurements using lock-in techniques have been carried out in a shielded He bath cryostat: special attention has been devoted to high-frequency filtering on the measurement wires to reduce the noise level on the junctions.

Received 19 March 2007; accepted 30 May 2008; published 29 June 2008.

References

- Norman, M. R. & Pepin, C. The electronic nature of high temperature cuprate superconductors. *Rep. Prog. Phys.* **66**, 1547–1610 (2003).
- Timusk, T. & Statt, B. The pseudogap in high-temperature superconductors: An experimental survey. *Rep. Prog. Phys.* **62**, 61–122 (1999).
- Ding, H. *et al.* Spectroscopic evidence for a pseudogap in the normal state of underdoped high- T_c superconductors. *Nature* **382**, 51–54 (1996).
- Norman, M. R. *et al.* Destruction of the Fermi surface in underdoped high- T_c superconductors. *Nature* **392**, 157–160 (1998).
- Renner, Ch., Revaz, B., Genoud, J.-Y., Kadowaki, K. & Fischer, O. Pseudogap precursor of the superconducting gap in under- and overdoped $\text{Bi}_2\text{Sr}_2\text{CaCu}_2\text{O}_{8+\delta}$. *Phys. Rev. Lett.* **80**, 149–152 (1998).
- Emery, V. J. & Kivelson, S. A. Importance of phase fluctuations in superconductors with small superfluid density. *Nature* **374**, 434–437 (1995).
- Randeria, M. in *Proc. Int. School of Physics 'Enrico Fermi' Course CXXXVI on High Temperature Superconductors* (eds Iadonisi, G., Schrieffer, J. R. & Chialfalo, M. L.) 53–75 (IOS Press, Amsterdam, 1998).
- Ferrell, R. A. Fluctuations and the superconducting phase transition: II. Onset of the Josephson tunneling and paraconductivity of a junction. *Low Temp. Phys* **1**, 423–442 (1969).
- Scalapino, D. J. Pair tunneling as a probe of fluctuations in superconductors. *Phys. Rev. Lett.* **24**, 1052–1055 (1970).
- Anderson, J. T. & Goldman, A. M. Experimental determination of the pair susceptibility of a superconductor. *Phys. Rev. Lett.* **25**, 743–747 (1970).
- Janko, B., Kosztin, I., Levin, K., Norman, M. R. & Scalapino, D. J. Incoherent pair tunneling as a probe of the cuprate pseudogap. *Phys. Rev. Lett.* **82**, 4304–4307 (1999).
- Barone, A. & Paterno, G. *Physics and Applications of the Josephson Effect* (Wiley–Intersciences, New York, 1982).
- Golubov, A. A. *et al.* Resonant tunneling in Y(Dy)Ba₂Cu₃O_{7- δ} /PrBa₂Cu_{3- δ} Ga₂O_{7- δ} /Y(Dy)Ba₂Cu₃O_{7- δ} ramp type Josephson junctions. *Physica C* **235–240**, 3261–3262 (1994).
- Bari, M. A. c -axis tunneling in YBa₂Cu₃O_{7- δ} trilayer junctions with PrBa₂Cu_{3- δ} Ga₂O_{7- δ} barrier. *Physica C* **256**, 227–235 (1996).
- Devyatov, I. A. & Kupriyanov, M. Yu. Resonant tunneling through SIS junctions of arbitrary size. *Zh. Eksp. Teor. Fiz.* **112**, 342–352 (1997); *JETP Lett.* **85**, 189–194 (1997).
- Yoshida, J. & Nagano, T. Tunneling and hopping conduction via localised states in thin PrBa₂Cu₃O_{7- δ} barriers. *Phys. Rev. B* **55**, 11860–11871 (1997).
- Glazman, L. I. & Matveev, K. A. Inelastic tunnelling across thin amorphous films. *Sov. Phys. JETP* **67**, 1276–1282 (1988).
- Kadin, A. M. & Goldman, A. M. Pair-field susceptibility and superconducting tunneling: A macroscopic approach. *Phys. Rev. B* **25**, 6701–6710 (1982).
- Devyatov, I. A. & Kupriyanov, M. Yu. Current–voltage characteristics of a SIS structures with localised states in the material of the barrier layer. *Zh. Eksp. Teor. Fiz.* **114**, 687–699 (1998); *JETP Lett.* **87**, 375–381 (1998).
- Takenaka, K., Mizuhashi, K., Takagi, H. & Uchida, S. Interplane charge transport in YBa₂Cu₃O_{7- δ} : Spin-gap effect on in-plane and out-of-plane resistivity. *Phys. Rev. B* **50**, 6534 (1994).
- Corson, J., Malozzi, R., Orenstein, J. J. N., Eckstein, J. N. & Bozovic, I. Vanishing of phase coherence in underdoped Bi₂Sr₂CaCu₂O_{8+ δ} . *Nature* **398**, 221–223 (1999).
- Xu, Z. A. *et al.* Vortex-like excitations and the onset of superconducting phase fluctuation in underdoped La_{2- x} Sr _{x} CuO₄. *Nature* **406**, 486–488 (2000).
- Wang, Y. *et al.* Onset of the vortex-like Nernst signal above T_c in La_{2- x} Sr _{x} CuO₄ and Bi₂Sr_{2- x} La _{x} CuO₆. *Phys. Rev. B* **64**, 224519 (2001).
- Rullier-Albenque, F. *et al.* Nernst effect and disorder in the normal state of high- T_c cuprates. *Phys. Rev. Lett.* **96**, 067002 (2006).
- Ussishkin, I., Sondhi, S. L. & Huse, D. A. Gaussian superconducting fluctuations, thermal transport, and the Nernst effect. *Phys. Rev. Lett.* **89**, 287001 (2002).
- Pourret, A. *et al.* Observation of the Nernst signal generated by fluctuating Cooper pairs. *Nature Phys.* **2**, 683–686 (2006).
- Carrington, A., Mackenzie, A. P., Lin, C. T. & Cooper, J. R. Temperature dependence of the Hall angle in single-crystal YBa₂(Cu_{1- x} Co _{x})₃O_{7- δ} . *Phys. Rev. Lett.* **69**, 2855–2858 (1992).
- Bergeal, N. *et al.* Using ion irradiation to make high- T_c Josephson junctions. *J. Appl. Phys.* **102**, 083903 (2007).

Acknowledgements

We acknowledge M. Grilli, S. Caprara, C. Castellani and C. Di Castro for stimulating discussions. We also thank P. Monod, O. Kaitasov and C. Dupuis.

Author information

Reprints and permission information is available online at <http://npg.nature.com/reprintsandpermissions>. Correspondence and requests for materials should be addressed to N.B. or J.L.